Equal Channel Angular Extrusion of AA 6063 Using Conventional Direct Extrusion Press

Cheng-Hsien Liu and Hsin-Chih Lin

In the present work, an extrusion-equal channel angular extrusion (Ex-ECAE) process composed of two processes, extrusion and ECAE, is developed. The Ex-ECAE die contains three segments and is used directly in the conventional direct extrusion press to refine the microstructure, specifically the coarse grain layer (CGL) on the surface of the extrudate. The first segment in the die is designed to perform the normal extrusion process and the second and third segments to perform the process of ECAE. The study reveals that the CGL can be eliminated (refined) completely at the macroscale. At the microscale, the original grain is subdivided into subgrain, which contains many smaller cells. The results can be explained by the grain subdivision mechanism. The textures of the Ex-ECAE sample at various segments are measured using EBSD (Electron Backscatter Diffraction). The results reveal that the first segment of the Ex-ECAE sample has a perfect fiber texture which consists of a mixture of strong $\langle 001 \rangle$ and weak $\langle 111 \rangle$ fiber components. The texture of the second segment is a mixture of strong (1 1 0) [1 −2 1] and weak (0 1 1) [2 −1 0] fiber components. However, the main component of the second segment is a typical texture of the "alloy" or "brass" type. Finally, the texture of the extrudate (the third segment) is reversed to an incomplete fiber texture which consists of strong (0 0 1) [−1 −1 0] and weak (1 1 1) [1 −1 0].

1. Introduction

Direct extrusion is a highly efficient process and is widely used to produce products or semi-products of aluminum alloys in industry. In the direct extrusion process, a preheated billet is placed in a heated container, and then a stem or ram protected by a dummy block presses the billet through a die with an opening in the shape of the desired profile. A loading method of billet-to-billet makes direct extrusion a continuous process. The deforming billet in the container is divided into three main regions, i.e., a primary deformation zone, a dead metal zone (DMZ), and an intense shear zone (Ref 1, 2). The materials that flow through the shear deformation zone will have a large shear strain. Under critical conditions (i.e., high strain/rate and high temperature), the discontinuous dynamic recrystallization will occur in the shear deformation zone. These intense shear-deformed materials will become the coarse grain layer (CGL) on the surface of the extrudate (Ref 3-8). The main reason causing the coarse grain layer on the surface of the extrudate is explained as follows. In practice, most of the extrudate of the aluminum alloys are quenched on-line, i.e., T5 treatment. For maximum solubility, the temperature of the billet is generally up to 480-490 °C. If the core temperature of extrudate is expected to reach the solution treatment temperature 530 °C at the exit, then due to the friction

effect the surface temperature of the extrudate will be far higher than 530 °C. Under such a high temperature, the recrystallized grains on the surface will grow rapidly and out of control. The extrudate with the CGL usually is regarded as an undesirable product that must be scrapped. A layer of coarse grains on or just under the surface of an extrusion can cause problems such as bending failure, orange peel finish, streaking, and variations in surface brightness (Ref 3).

Usually, the CGL is removed by machining or eliminated by thermomechanical treatment (TMT). However, these methods will result in lower productivity and increased costs. In the present study, the concept of the equal channel angular extrusion (ECAE) will be introduced to design the extrusion die. Among the Severe Plastic Deformation (SPD) techniques, ECAE is known to be a simple but highly effective process for refining the microstructure of metal and alloys (Ref 9-14). According to the Hall-Petch equation, the yield strength of the material will increase as the grain size is reduced. In the ECAE process, a preheated and well-lubricated billet is pressed into a die that is composed of two channels of equal cross-sectional areas that meet at an angle which usually is at 90° or 120°. There are three main characteristics of the ECAE process: (1) hydrostatic stress state, (2) abrupt changes in the strain path, and (3) An insignificant change in the dimension of the billet after the ECAE process. Therefore, the ECAE process can be repeated many times to impose a billet of a large plastic strain and obtain the highest dislocation density. Under ideal conditions, the deformation of the billet during the ECAE process is confined to a narrow zone at the plane, which is usually referred to as a shear plane, of the intersection of the two die's channels. The stress state at the shear plane approximates a simple shear (Ref 9-14).

In the present work, we perform ECAE using a conventional direct extrusion press, named extrusion-ECAE (Ex-ECAE). The die of the Ex-ECAE is schematically shown in Fig. 1, which displays one of the half parts. The half die plane shown in Fig. 1 is referred to as a parting plane. The channel in the die

Cheng-Hsien Liu and **Hsin-Chih Lin**, Department of Materials Science and Engineering, National Taiwan University, 1, Roosevelt Road, Sec. 4, Taipei 10617, Taiwan. Contact e-mail: hclinntu@ntu.edu.tw.
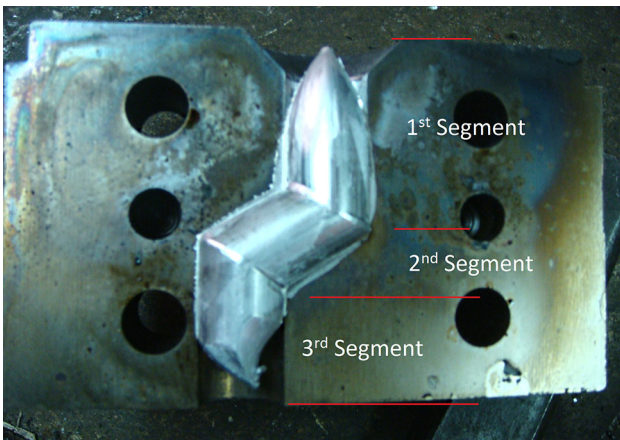
Fig. 1 One-half of the designed Ex-ECAE die used in the present study. A sample left in the channel after the Ex-ECAE is also shown. The die angle is 120°, and the diameter of the channel is 20 mm

of the Ex-ECAE contains three segments. The first segment is equivalent to the conventional direct extrusion. A conical entrance is designed to have the function of a package die. From the view of the ECAE, an ongoing, continuous, and long "extruded" billet is pressed into the die (i.e., the second and third segments), and the product is constantly output in the Ex-ECAE process. The combination of the second and third segments is equivalent to the ECAE process via route C. Therefore, the 'billet' for the ECAE process is quite long, and it is not necessary to rotate the billet between the passes. However, it becomes possible to have an Ex-ECAE extrudate with any shape. Thus, "billet" of any shape can perform the ECAE process without requiring shaping in advance.

The deformation conditions of the Ex-ECAE and the ECAE are quite different. (1) The extrusion speed in the ECAE section of the Ex-ECAE is much higher than in the ECAE. (2) The initial dislocation structures of the 'billet' are different. In the ECAE, the billet is usually annealed, so the dislocation density is lower. In the Ex-ECAE, the billet comes from the extrudate, the initial dislocation density is higher, and it depends on the extrusion ratio and temperature. (3) In the ECAE, the billet is well lubricated. In the direct extrusion process, the billet usually is not lubricated to avoid contaminating the extrudate. Therefore, in the Ex-ECAE, the friction between the extrudate and the channel is higher than in the ECAE. Bowen et al. (Ref 10) have analyzed the deformation behavior of the billet in the ECAE and shown that the strain achieved and the homogeneity depends on the friction conditions and the application of a back pressure, etc. With low friction and a lack of back pressure, the deformation zone at the shear plane will spread through an arc, and the billet has a greater tendency to become partially bent. Thus, it leads to a lower overall shear strain compared to the theoretically expected one for a simple shear. Additionally, the inhomogeneously deformed area of the billet will be increased. It is expected that in the Ex-ECAE the friction of the exit channel will act similarly to the back pressure and constrain the arc length of the deformation zone (Ref 15) (i.e., the corner of the channel will be filled with materials).

Finally, it is well known that a heavily deformed material usually contains a strong texture. However, texture is not a desired phenomenon for most structural material applications. Therefore, it is quite important to understand the texture of the

product for structural applications. In the present study, the microstructure evolution of the Ex-ECAE rod is investigated systematically. Meanwhile, the textures of the Ex-ECAE sample at various segments are measured using EBSD. And the CODF (Continuous Orientation Distribution Function) is used to exhibit the measured results of the textures.

2. Experimental Procedures

The AA 6063 billet of an 88.9-mm diameter was cast using the direct chill casting process. Then the billet was subjected to homogenization treatment at temperature of 470 °C for 8 h. After homogenization, the 250-mm-long billet was cut and preheated to 250 °C. The drawing of the designed Ex-ECAE die is shown in Fig. 2. Although the accumulated strain is directly related to the pass number, considering the issue of the capacity of the extrusion press and the arrangement of the production line, the die only contains two passes, and the strain path of route C is selected. However, Zhang et al. (Ref 16) analyzed the plastic deformation zone in multi-pass ECAP at high temperature (450 °C) and suggested that because of the reverse direction, route C will develop a stable deformation zone.

The temperature of both the Ex-ECAE die and the container was set at 200 °C. During the Ex-ECAE process, the ram speed was fixed at 1.5 mm/s. The diameter of the extrudate was 20 mm. Therefore, the speed of the extrudate flow through the channel was about 30 mm/s. After the Ex-ECAE process was finished, the material left in the channel, which was named the Ex-ECAE sample, was cooled down to room temperature in the die. Then the Ex-ECAE sample was cut along the parting plane. After polishing, the parting plane of the Ex-ECAE sample was immersed in 10% NaOH solution for 20 min at room temperature to reveal the macrostructure and the flow pattern of material.

The TEM specimens were sampled from the transverse cross sections of the Ex-ECAE samples at three segments. The TEM specimen was ground to a thickness of 130 μm and then twin-jet polished in a 30% HNO_3 + 70% CH_3OH solution at −40 °C and 25 V. These specimens were examined using a FEI Tecnai G2 F20 transmission electron microscope operating at 200 kV.

The EBSD specimens were sampled from the core of billet and the Ex-ECAE sample in the transverse cross section at various segments to measure the textures. And then these specimens were twin-jet polished in a 30% HNO_3 + 70% CH_3OH solution at 243 K (−30 °C) and at 20 V. The EBSD and CODF analyses were carried out using a system of NOVA NANO SEM 450 + EDAX/EBSD.

3. Experimental Results and Discussion

3.1 Macrostructure of the Ex-ECAE Rod

The press load needed to perform the Ex-ECAE process is expected to be quite high. The appearance of the extruded rod is consistent with the expected high load needed. As shown in Fig. 3, a longitudinal parting line appears at the bottom of the photo. Additionally, the whole surface of the rod is covered by transverse and periodic wave marks. These surface characteristics illustrate the high press load and the existence of high friction between the die and the material during the Ex-ECAE
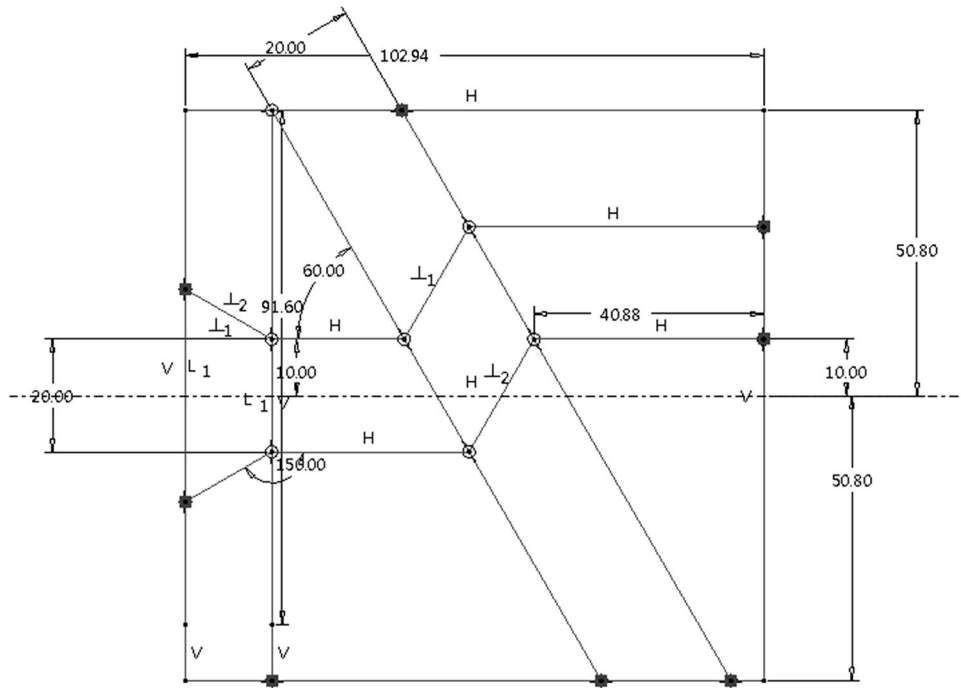
Fig. 2 Schematic drawing of the designed Ex-ECAE die that is composed of three segments
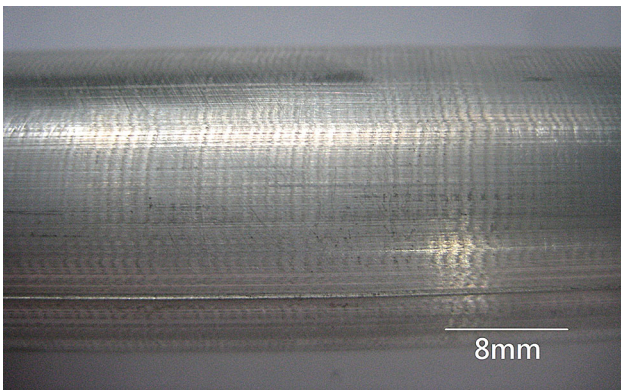

Fig. 3 Transverse and periodic wave marks cover the whole surface of the Ex-ECAE rod. The longitudinal line that appears at the bottom of the extrudate is the parting line

Fig. 4 Macrostructure and flow pattern of the Ex-ECAE sample at various segments

process. However, when these wave marks were examined under SEM, no microcracks were seen. From the direct extrusion view, the 'bearing length' of designed Ex-ECAE die is too long, and the friction resistance increases. This will cause both the load needed to extrude and the surface temperature of the extrudate to increase.

Figure 4 shows the macrostructure and flow pattern of the Ex-ECAE sample at various segments. There is a CGL produced on the surface of the extrudate at the first segment. This phenomenon occurs usually in the aluminum extrusion industry. Aluminum alloys are high stacking fault energy alloys, and dynamic recovery is the dominant mechanism used to reduce the stored energy during the plastic deformation. However, under severe conditions, such as a high strain rate on the surface of the extrudate, high plastic strain, and high temperature, the dynamic recovery will be replaced by discontinuous dynamic recrystallization. Also, due to the high
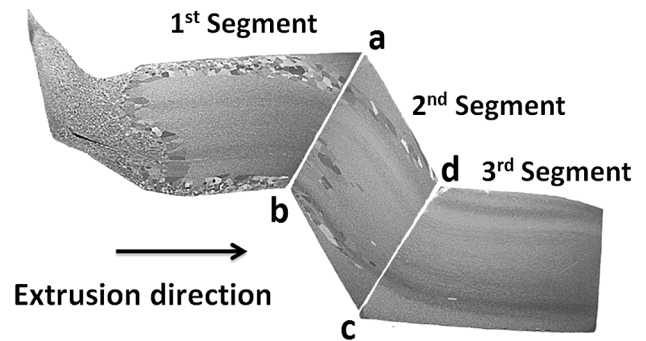
temperature the recrystallization is completed very soon, and uncontrolled grain growth occurs. The large plastic strain (The effective strain imposed on the extrudate in the first segment is 2.932) deformation results in the development of fibrous microstructures in the core region, which are aligned parallel to the extrusion direction. The overall macrostructure of the first segment is the typical structure observed in the direct extrusion.

Prangnell et al. (Ref 17) have predicted using FEM (Finite Element Method) analysis that with the friction of the channel in the ECAE die, the metal appears to fill the internal corner of the die. Upon entering the second segment, the DMZ at the corners (i.e., a, b, c, and d) are formed. By observing the flow pattern, one can determine the CGLs (top and bottom) along the DMZ flow into the next segment and how they form an arc path. As the flow proceeds, the CGL becomes narrow. The CGL of the top disappears as it reaches DMZ d. Additionally, the bottom one disappears before it flows into the third segment. The arc path is not symmetrical to the shear plane, i.e., the intersect plane of the channels. The formation of the
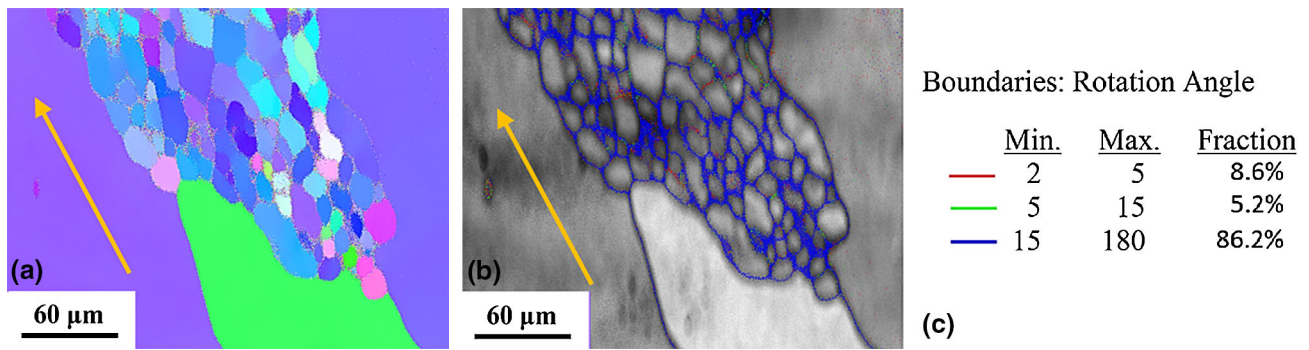
Fig. 5 One of the grains in the CGL is subdivided into many fine grains as the CGL flow into the next segment. (a) EBSD image. (b) and (c) Grain boundary measurement. The orange arrow indicates the direction of the materials flow
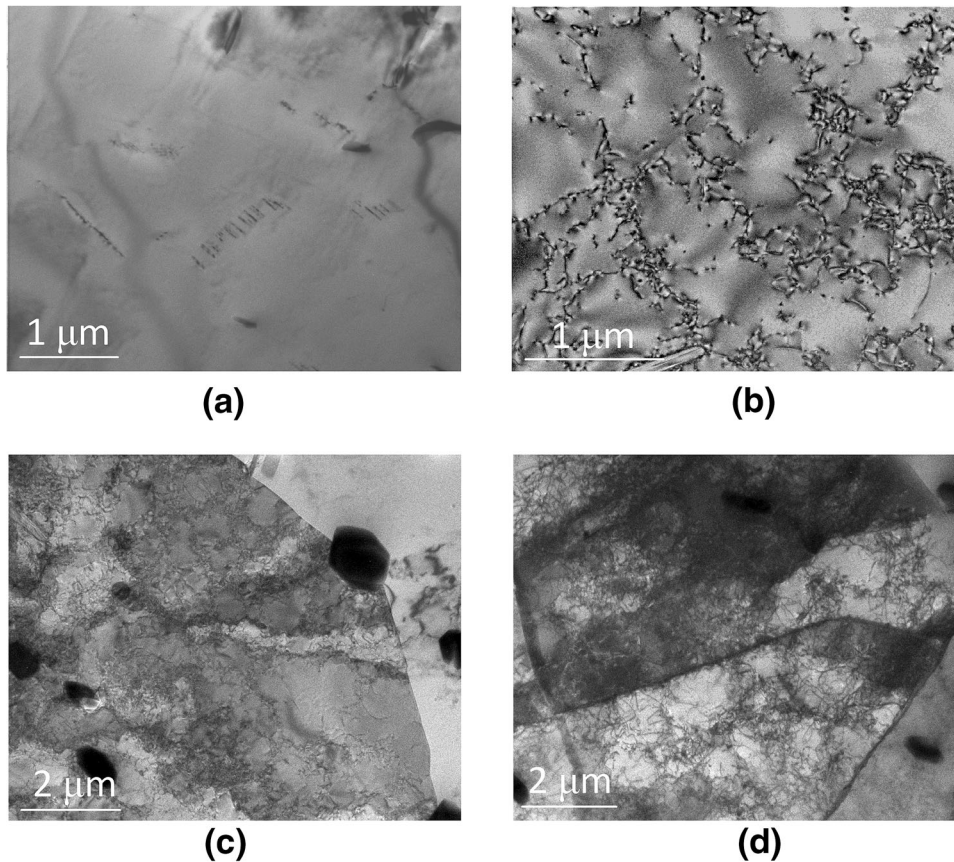

Fig. 6 The evolution of the dislocation structures at various segments during Ex-ECAE process. (a) Billet. (b) The first segment. (c) The second segment. (d) The third segment

asymmetric flow results from that the DMZs, e.g., d and a, are too close. It implies that the length of the second segment is too short. However, the result is that the CGLs do not flow back to the surface of the extrudate as they flow into the second and third segments. As a consequence, the CGLs will undergo an intense shear deformation due to the friction induced velocity difference across the cross section of the channel.

The equiaxed grains with a diameter of 0.68-2 mm become more longitudinal as the CGL flows into next segment. A specimen was sampled from the CGL near the DMZ b, as shown in Fig. 4, to observe the subdivision of the coarse grains. The EBSD observation shown in Fig. 5(a) illustrates that one of the

coarse longitudinal grains in the CGL is subdivided into many fine grains under the intense shear deformation. The flow direction of the CGL is indicated by the orange arrow. These continuous dynamic recrystallized grains have a diameter of 15.5-25.8 μm. And about 86% of these new grains are bounded by high-angle grain boundaries, as shown in Fig. 5(b) and (c). The disappearance (refinement) of the CGL can be explained by grain subdivision, i.e., the microstructural and texture mechanism (Ref 18-20). The refinement of the CGL located at the bottom is more effective than one at the top. This should result from more of simple shear strain imposed on the CGLs of bottom at the corner b than that of top at the corner a (Ref 15, 21).
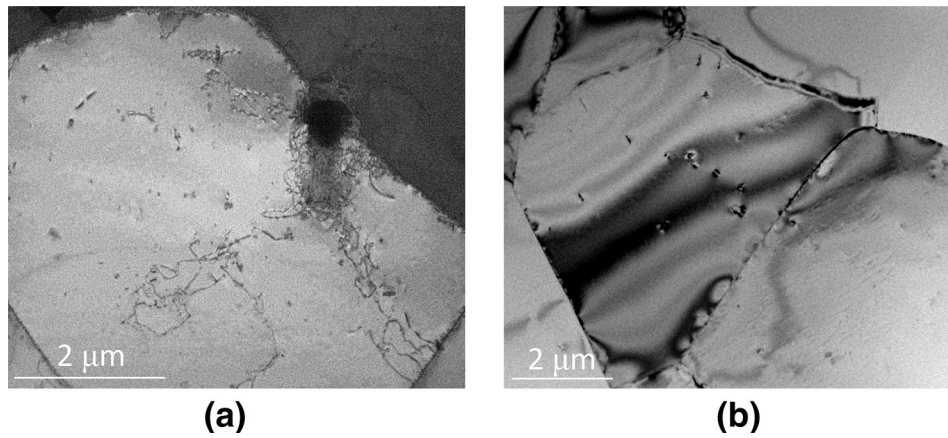
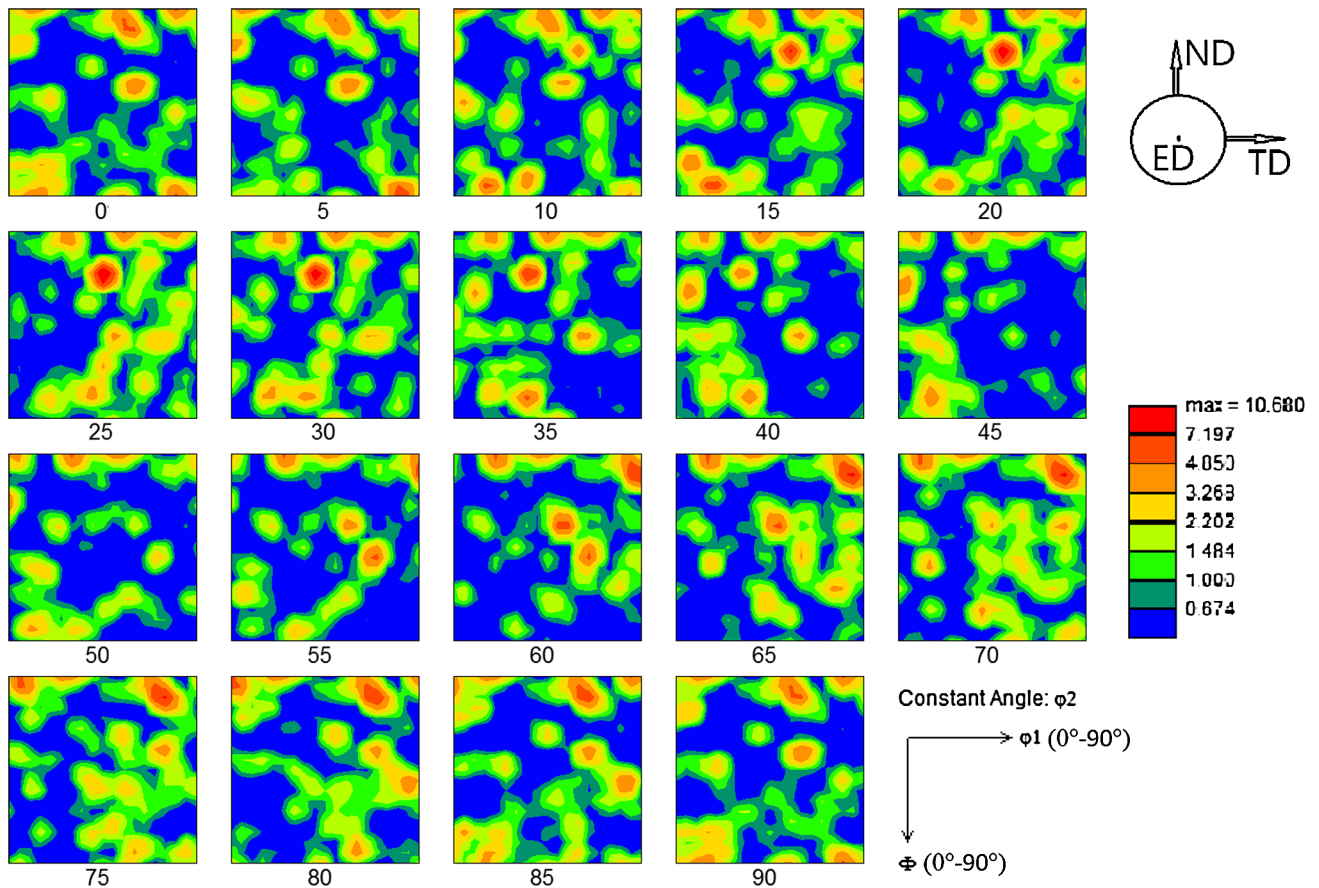**Fig. 7** The dislocation structures of (a) annealed and (b) An-ECAE rods

Fig. 8 The CODF image of the billet used in the present study

3.2 Microstructure Evolution of the Ex-ECAE Rod

To illustrate the microstructural evolution of the Ex-ECAE, the specimens of the transverse section are sampled and observed under TEM. The billet used in this study is DC cast and homogenized. The microstructure is shown in Fig. 6(a). We observe that the dislocation density is quite low, and only a few arrays of split dislocations are occasionally visible. During the extrusion deformation (the first segment), the dislocation density quickly increases. Due to the large plastic strain, as

mentioned above, that is imposed and the high stacking fault energy of aluminum alloys, the cellular structure develops, as shown in Fig. 6(b). The dimensions of the cells are about $2 \times 1 \ \mu m^2$. The cell structure is believed to form in advance at the first segment, which is helpful for the grain refinement of subsequent processes, i.e., the second and third segments (ECAE via route C). However, the dislocation density in the cell wall is not high. During the ECAE process (the second segment), there are two cell sizes that appear as shown in
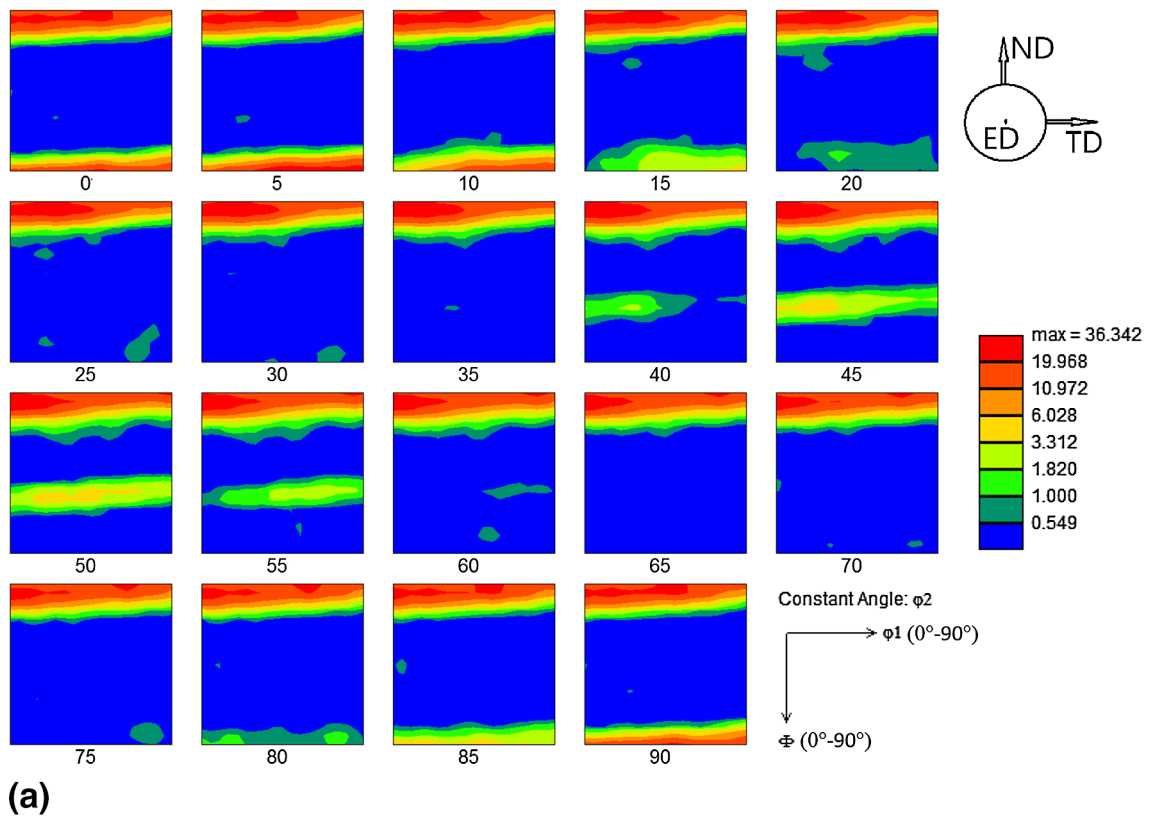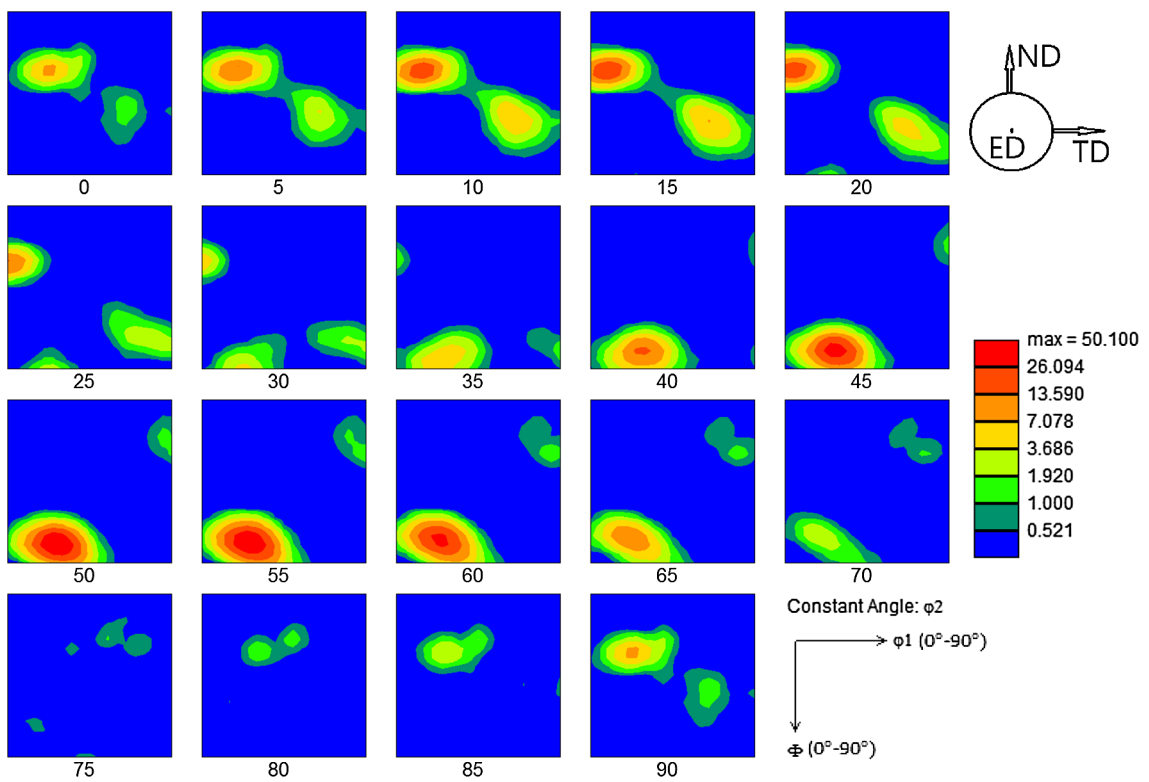
Fig. 9 The CODF of the Ex-ECAE sample at various segments in the Ex-ECAE process. (a) The first segment. (b) The second segment. (c) The third segment
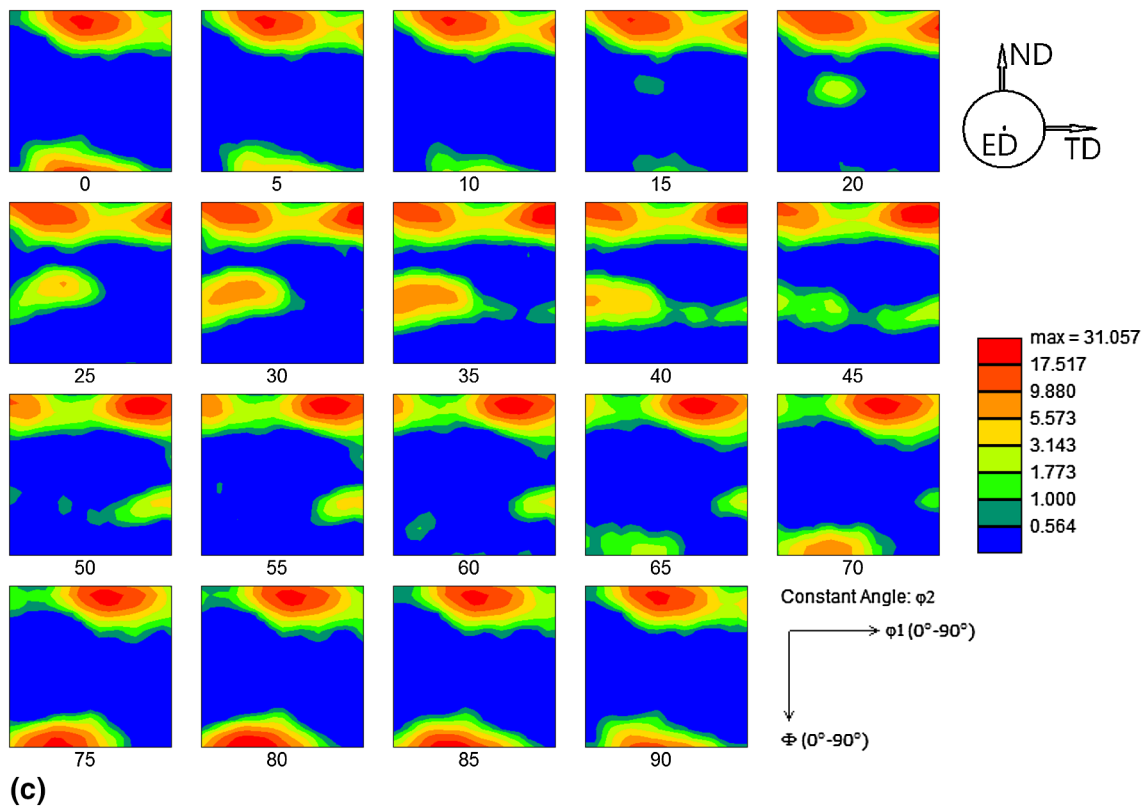
Fig. 9 continued

Fig. 6(c). The larger one (about 8×3 μm) has boundaries composed of a high dislocation density, and they become quite clear as the Ex-ECAE process is completed (at the third segment), as shown in Fig. 6(d). Within these subgrains, the smaller cells are covered. These cells become the precursors that re-subdivide the subgrains if there is further plastic strain that is imposed.

For a comparison, a rod from conventional direct extrusion is annealed at 410 °C and put at the first segment of the channel in advance. Then it is pressed through the channel by the rod extruded from the billet during the Ex-ECAE process. Therefore, the annealed rod undergoes the ECAE via the route C process only and is referred to as an An-ECAE sample. The microstructures of the annealed and the An-ECAE rods are shown in Fig. 7. After annealing the microstructure of the rod, subgrains form, and there are no signs of recrystallization, as shown in Fig. 7(a). The annealed rod is believed to undergo a large number of dynamic recoveries during the extrusion deformation, and the driving force of the static recrystallization decreases significantly during annealing. However, Fig. 7(a) reveals the dislocation density of the annealed rod is lower than the first segment of the Ex-ECAE (Fig. 6b). Figure 7(b) reveals the microstructure of the An-ECAE, which is quite different from the Ex-ECAE (Fig. 6d). No dislocation can be found within the subgrain of the An-ECAE. According to the grain subdivision model proposed by Meyers (Ref 19), the microstructure of Fig. 6(d) re-subdivides the existing subgrain. Thus using an Ex-ECAE die, the extrusion process (the first segment) is useful for microstructural refinement. Another important factor for using the Ex-ECAE process is the material flow speed in the die channel, which is much higher than for

conventional ECAE. As mentioned above, in this study the ram speed is 1.5 mm/s, and then the material flow rate in the channel is 30 mm/s. It is expected that the adiabatic simple shear deformation in the Ex-ECAE process will increase the temperature of the material. The activation of the dislocation in the dynamic recovery process will be easier as the temperature increases.

3.3 Texture Evolution of the Ex-ECAE Rod

As mentioned above, the Ex-ECAE process is composed of two processes—direct extrusion and ECAE via route C. The extrusion process is an axisymmetric deformation process, but the ECAE process is a simple shear deformation process (Ref 9). Therefore, the final texture of the third segment (or the extrudate) of the Ex-ECAE sample should be determined by the simple shear deformation. The texture of a simple shear deformed specimen is usually indexed in the form—plane of shear/direction of shear (Ref 22-26). However, in practice it is more convenient to index the texture of a long bar in the form—plane of the transverse cross section/direction of radius. Therefore, in the present study the texture is indexed in the form—plane of the transverse cross section of the sample/ direction of the normal of the die's parting plane.

The CODF of the billet used in the present work is shown in Fig. 8. It presents clearly that the texture of the billet can be regarded as random, due to the use of the Al-Ti-B grain refiner wire during direct-chilled (DC) casting (Ref 27). The use of the grain refiner results in the growth direction of the nuclei which is not influenced by the heat flow. Therefore, the billet contains equiaxed grains with random orientation. The grain size of the

Table 1 Summarization of the Euler angles and texture index of the samples at various segments in the Ex-ECAE process

Samples	Euler angles $(\varphi_1, \Phi, \varphi_2)$	Texture index/intensity
The first segment	Fiber texture	$\langle 0\ 0\ 1 \rangle$ Strong
		$\langle 1\ 1\ 1 \rangle$ Weak
The second segment	(26, 79.8, 50)	(1 1 0) [1 −2 1]/48.6×
	(9.4, 32.6, 15)	(0 1 1) [2 −1 0]/21×
The third segment	(76.2, 6, 50)	(0 0 1) [−1 −1 0]/25.4×
	(5.4, 54.8, 35)	(1 1 1) [1 −1 0]/8.9×

billet is approximately 200 μm. The CODF images of the Ex-ECAE sample at various segments are shown in Fig. 9. And all of the Euler angles and texture indexes are summarized in Table 1. As expected, the first segment of the Ex-ECAE sample exhibits a perfect fiber texture, as shown in Fig. 9(a), due to the axisymmetric deformation mode of the extrusion process. The texture of the first segment consists of the expected mixture of strong $\langle 0\ 0\ 1 \rangle$ and weak $\langle 1\ 1\ 1 \rangle$ fiber components. This is a typical fiber texture that often occurs in the wire drawing process of FCC metals and alloys (Ref 22).

As the first segment of the Ex-ECAE sample flows into the second segment, the deformation mode changes from axisymmetric deformation mode to simple shear deformation mode. Then the fiber texture is destroyed and a new texture is developed by the simple shear deformation. As shown in Fig. 9(b), the second segment has a texture which consists of two components with different intensities. The main component is (1 1 0) [1 −2 1] and the weak one is (0 1 1) [2 −1 0]. However, the texture of main component is the well-known "alloy-" or "brass-" type texture (Ref 22). The texture of the third segment, as shown in Fig. 9(c), is also a mixture of two components—the strong component (0 0 1) [−1 −1 0] and the weak component (1 1 1) [1 −1 0]. However, it is worth noting that the iso-intensity curve of the main component in Fig. 9(c) spreads discontinuously along $\Phi = 0°$ and 90°. It means that the third segment exhibits an incomplete fiber texture. The ECAE via route C is a reverse process because the shear stress is reversed on the same shear plane between the passes (Ref 22). It implies that the texture of the second segment will be reversed to one of the first segment as it flows into the third segment. However, the deformation mode between the direct extrusion and ECAE is quite different. The fiber texture is difficult to be completely recovered in the third segment. In the present study, there are only two passes of ECAE in the Ex-ECAE die. It is expected that the more passes the Ex-ECAE die has, the less recovery of the fiber texture will be.

4. Conclusions

An Ex-ECAE process composed of two processes, extrusion and ECAE, is developed. The Ex-ECAE die contains three segments and is used directly in the conventional direct extrusion press to refine the microstructure, Specifically the CGL on the surface of the extrudate. The results reveal that the CGL can be eliminated (refined) completely at the macroscale. The CGL is eliminated mainly by the formation of an asymmetric arc path flow at the corner of the die channel. This asymmetric path flow

causes the CGL to flow under the subsurface of the channel instead of flowing back to the surface of the channel, and then the flow velocity difference induced by the friction across the cross section results in the CGL flowing through an intense shear deformation zone. At the microscale, the original grain is subdivided by subgrain that contains many smaller cells. The results can be explained by the grain subdivision mechanism.

However, in the first segment of the Ex-ECAE process, the as-extruded billet with a high dislocation density is notably helpful for the grain refinement in the subsequent ECAE process (the second and third segments). The textures of the Ex-ECAE sample at various segments have been analyzed by EBSD and CODF images. The final texture of the extrudate is a mixture of the strong component (0 0 1) [−1 −1 0] and the weak component (1 1 1) [1 −1 0]. The continuous mass production of the ECAE may be achieved by the Ex-ECAE process. Extrudates with any shapes can be produced first by the extrusion process (the first segment) and then grain refined further by the subsequent ECAE process.

References

1. M. Bauser, G. Sauer, and K. Siegert, *Extrusion*, 2nd ed., ASM International®, Materials Park, 2006, p 68
2. T. Sheppard and S.J. Paterson, Some Observations on Metal Flow and the Development of Structure During the Direct and Indirect Extrusion of Commercial Purity Aluminium, *J. Mech. Work. Technol.*, 1982, **7**(1), p 39–56
3. Coarse Grain Surface Layer in 6000 Series Extrusions, http://sales.riotintoaluminium.com/document_get.aspx?id=143
4. M. Schikorra, L. Donate, L. Tomesani, and A.E. Tekkaya, Microstructure Analysis of Aluminum Extrusion: Grain Size Distribution in AA6060, AA6082 and AA7075 Alloys, *J. Mech. Sci. Technol.*, 2007, **21**(10), p 1445–1451
5. W.H. Van Geertruyden, W.Z. Misiolek, and P.T. Wang, Surface Grain Structure Development During Indirect Extrusion of 6xxx Aluminum Alloys, *J. Mater. Sci.*, 2005, **40**(14), p 3861–3863
6. W. Libura and J. Zasadzinski, The Influence of Strain Gradient on Material Structure During Extrusion of the AlCu4 Mg Alloy, *J. Mater. Process. Technol.*, 1992, **34**(1–4), p 517–524
7. Pawel Kazanowski, Heather M. Browne, Wojciech Libura, and Wojciech Z. Misiolek, Mechanical and Microstructural Performance of Convex Dies in Axisymmetric Extrusion—Theory and Experimental Verification, *Mater. Sci. Eng., A*, 2005, **404**(1–2), p 235–243
8. Xinjian Duan and Terry Sheppard, Simulation and Control of Microstructure Evolution During Hot Extrusion of Hard Aluminium Alloys, *Mater. Sci. Eng. A*, 2003, **351**(1–2), p 282–292
9. V.M. Segal, Materials Processing by Simple Shear, *Mater. Sci. Eng. A*, 1995, **197**(2), p 157–164
10. Y. Iwahashi, Z. Horita, M. Nemoto, and T.G. Langdon, An Investigation of Microstructural Evolution During Equal-Channel Angular Pressing, *Acta Mater.*, 1997, **45**(11), p 4733–4741
11. Y.T. Zhu and T.C. Lowe, Observations and Issues on Mechanisms of Grain Refinement During ECAP Process, *Mater. Sci. Eng. A*, 2000, **291**(1–2), p 46–53
12. U. Chakkingal and R.F. Thomson, Development of Microstructure and Texture During High Temperature Equal Channel Angular Extrusion of Aluminium, *J. Mater. Process. Technol.*, 2001, **117**(1–2), p 169–177
13. Saiyi Li, Irene J. Beyerlein, and Carl T. Necker, On the Development of Microstructure and Texture Heterogeneity in ECAE Via Route C, *Acta Mater.*, 2006, **54**(5), p 1397–1408
14. Yoshinori Iwahashi, Jingtao Wang, Zenji Horita, Minoru Nemoto, and Terence G. Langdon, Principle of Equal-Channel Angular Pressing for the Processing of Ultra-Fine Grained Materials, *Scripta Mater.*, 1996, **35**(2), p 43–146
15. J.R. Bowen, A. Gholinia, S.M. Roberts, and P.B. Prangnell, Analysis of the Billet Deformation Behaviour in Equal Channel Angular Extrusion, *Mater. Sci. Eng. A*, 2000, **287**(1), p 87–99

16. Z.J. Zhang, I.H. Son, Y.T. Im, and J.K. Park, Finite Element Analysis of Plastic Deformation of CP-Ti by Multi-Pass Equal Channel Angular Extrusion at Medium Hot-Working Temperature, *Mater. Sci. Eng. A*, 2007, **447**(1–2), p 134–141

17. P.B. Prangnell, C. Harris, and S.M. Roberts, Finite Element Modelling of Equal Channel Angular Extrusion, *Scripta Mater.*, 1997, **37**(7), p 983–989

18. D.A. Hughes and N. Hansen, High Angle Boundaries Formed by Grain Subdivision Mechanisms, *Acta Mater.*, 1997, **45**(9), p 3871–3886

19. Marc A. Meyers, Vitali F. Nesterenko, Jerry C. LaSalvia, and Qing Xue, Shear Localization in Dynamic Deformation of Materials: Microstructural Evolution and Self-organization, *Mater. Sci. Eng. A*, 2001, **317**(1–2), p 204–225

20. P.L. Sun, P.W. Kao, and C.P. Chang, High Angle Boundary Formation by Grain Subdivision in Equal Channel Angular Extrusion, *Scripta Mater.*, 2004, **51**(6), p 565–570

21. A. Gholinia, P. Bate, and P.B. Prangnell, Modelling Texture Development During Equal Channel Angular Extrusion of Aluminium, *Acta Mater.*, 2002, **50**(8), p 2121–2136

22. U.F. Kocks, C.N. Tomé, and H.R. Wenk, *Texture and Anisotropy: Preferred Orientations in Polycrystals and Their Effect on Materials Properties*, 1st ed., Cambridge University Press, Cambridge, 1998, p 178–242

23. W.H. Huang, L. Chang, P.W. Kao, and C.P. Chang, Effect of Die Angle on the Deformation Texture of Copper Processed by Equal Channel Angular Extrusion, *Mater. Sci. Eng. A*, 2001, **307**, p 113–118

24. M. Haouaoui, K.T. Hartwig, and E.A. Payzant, Effect of Strain Path on Texture and Annealing Microstructure Development in Bulk Pure Copper Processed by Simple Shear, *Acta Mater.*, 2005, **53**, p 801–810

25. C. Pithan, T. Hashimoto, M. Kawazoe, J. Nagahora, and K. Higashi, Microstructure and Texture Evolution in ECAE Processed A5056, *Mater. Sci. Eng. A*, 2000, **280**, p 62–68

26. I.J. Beyerlein, R.A. Lebensohn, and C.N. Tomé, Modeling Texture and Microstructural Evolution in the Equal Channel Angular Extrusion Process, *Mater. Sci. Eng. A*, 2003, **345**, p 122–138

27. J. Hirsch, Texture and Anisotropy in Industrial Applications of Aluminum Alloys, *Arch. Metall. Mater.*, 2005, **50**(1), p 21–34